

# A MANUFACTURABILITY-BASED METHOD OF TOPOLOGICAL SHAPE OPTIMIZATION FOR STRUCTURES UNDER MULTIPLE LOADING CASES

HAO LI<sup>\*</sup>, LIANG GAO<sup>\*</sup>, LI ZHANG<sup>\*</sup> AND TAO WU<sup>†</sup>

<sup>\*</sup> School of Mechanical Science & Engineering  
Huazhong University of Science and Technology  
Luoyu Road 1037, Wuhan, Hubei, China  
e-mail: [gaoliang@mail.hust.edu.cn](mailto:gaoliang@mail.hust.edu.cn)

<sup>†</sup> School of Software Engineering  
Huazhong University of Science and Technology  
Luoyu Road 1037, Wuhan, Hubei, China  
e-mail: [wutaooptal@126.com](mailto:wutaooptal@126.com)

**Key Words:** *Topological Shape Optimization, Manufacturability, Extrusion, Level Set, Discrete Wavelet Transform.*

**Abstract.** Considering the manufacturability during the design phase, this paper proposes a level set-based method for the optimal design of extrudable structures under multiple loading cases. Firstly, the level set model is used to describe the moving structural boundary as the embedded zero level set. To avoid the mathematically solving of the difficult Hamilton-Jacobi equation, the compactly supported radial basis function (CSRBF) as well as the discrete wavelet transform (DWT) are introduced to transform the standard level set method into a parametric one, to which several well-established gradient-based algorithms can be applied. Besides, the linear system for the interpolation is extremely sparse in our study, which will guarantee the computational efficiency. Secondly, the multi-objective optimization considering different loading cases is formulated by a normalized exponential weighted criterion (NEWC) method. The NEWC is used to depict the entire Pareto set on both convex and non-convex Pareto frontier. Thirdly, a cross section projection strategy is utilized to satisfy the extrusion constraint and reduce the computational cost. Several numerical examples in 3D are provided to show the efficiency of the proposed method. The results verify this method can achieve a manufacturable design using lower computer effort.

## 1 INTRODUCTION

Topology optimization has long been identified as the most challenge topic among the structural optimization [1]. It is often used to help the designers with the distributing of materials in a given design domain during the conceptual design phase. However, knowing where to place the “solid” and “void” is not obvious, requiring complex optimization procedures. Intensive interests in topology optimization have been motivated by the

effectiveness in reducing product mass and improving structural performance. As a result, many methods have been established for solving a variety of topological optimization design problems, such as the homogenization method [2], the solid isotropic material with penalization (SIMP) approach [3,4], the evolutionary structural optimization (ESO) method [5] and the level-set based method [6-8] etc. Although the former three methods have got their own advantages in different aspects, they share a common drawback that the optimal structure boundary is relied on the shapes and numbers of the finite elements, and one may always observe a zigzag or vague boundary, consequently. This causes the obstacle to the identification of structural boundary in further detail design phase, and makes difficulties in the boundary-related optimization problems. The level set method is developed to conquer this troublesome defect.

Sethian and Wiegmann [6] are among the first few researchers who introduced conventional level set method to track and model the moving boundary with shape and topology changes in the field of structural optimization. Since then, a number of works [7-9] have been presented with the highlight of integrating the shape sensitivity into the level set-based framework on a fix Eulerian mesh. The great potential of the level set method is that it has the powerful capacity of flexible handling the topological changes and precise representing the smooth boundary. However, directly implementing the standard level set method is not an easy task, due to that several complicated numerical schemes, such as upwind scheme, extension velocities and reinitialization, are required to solve the PDEs.

The parametric formulation is regarded as one of the solutions for the numerical difficulties in the standard level set approach [10]. It approximates the time-dependent implicit level set function with CSRBFs [11]. The parametric level set method can inherit all the favourable features of the conventional level set method, and avoid the direct solving of Hamilton-Jacobi PDEs. In fact, the corresponding linear system in RBF interpolation will cost  $O(N^3)$  floating-point operations and  $O(N^2)$  memory requirement during processing. When the value of  $N$  gets large, it will lead to numerical instability, and one will failure to complete the optimization procedure within a reasonable computational time.

On the other hand, when topology optimization methods are applied to improve the performance of structure, another critical factor of a structure – manufacturability – also needs to be intentionally considered. In fact, if the manufacturability is not considered early in the design circle, the “optimal” product may not be fabricated by the modern manufacturing technology. Extrusion is a low-cost manufacturing technique to generate long products with constant cross sections. It often minimizes the cost of secondary machining. The manufacturing requirement for this process is that the design should keep a constant cross section. To this end, several particular schemes are developed to satisfy this manufacturing constraint [9,12-14]. Unfortunately, most of them are based on the elementary density methods, in which the optimal topologies are difficult to be extracted.

To the best of the authors’ knowledge, there are only a limited amount of public studies about using the level set-based method to solve manufacturability-based topology optimization problems. Therefore, this paper will propose an effective level set-based parameterization method for the optimization of structures considering the manufacturability as well as the multiple loading cases.

## 2 LEVEL SET-BASED BOUNDARY REPRESENTATION

### 2.1 Implicit Boundary Representation

In the present method, the higher-dimensional level set function is employed to describe the smooth boundary via the implicit representation. For instance, a 2D structure boundary is described by implicitly embedding it into the zero iso-surface of a relative 3D scalar function that is defined on fixed Eulerian rectilinear grids. In the level set model, different parts of structure are defined respectively as:

$$\begin{cases} \Phi(\mathbf{x}) > 0 \Leftrightarrow \forall \mathbf{x} \in \Omega \setminus \partial\Omega & \text{(Solid)} \\ \Phi(\mathbf{x}) = 0 \Leftrightarrow \forall \mathbf{x} \in \partial\Omega \cap D & \text{(Boundary)} \\ \Phi(\mathbf{x}) < 0 \Leftrightarrow \forall \mathbf{x} \in D \setminus \Omega & \text{(Hole)} \end{cases} \quad (1)$$

where  $D$  is the design domain including all admissible shapes  $\Omega$ , and  $\Phi$  is the level set function.

The propagation of structural boundary during iteration is governed by the Hamilton-Jacobi PDEs, via the introducing of pseudo-time  $t$ :

$$\frac{\partial\Phi(\mathbf{x}, t)}{\partial t} + \mathbf{V}_n(\mathbf{x})|\nabla\Phi(\mathbf{x}, t)| = 0 \quad (2)$$

here,  $\mathbf{V}_n$  represents the normal velocity vector on the boundary. The variation of level set surface is handled by the velocity in Hamilton-Jacobi equation.

Despite the several favorable characteristics with the implicit boundary representation, as mentioned previously, moving the boundary through the Hamilton-Jacobi PDEs is complicated [7,10]. As a result, more efficient parametric model with CSRBFs and DWT approximation is developed.

### 2.2 CSRBF-based Parametric Model

The RBFs are widely used as an effective tool to interpolate scattered data, and interest in this method exploded recently, such as in the fields of estimating partial derivatives and solving PDEs. It is represented by a family of radially-symmetric functions centered at a particular point. Compare with the globally supported RBFs, the CSRBFs lead to a sparse collection matrix, and has the merit of positive definiteness, which make it is suitable for the interpolation of level set function in topology optimization. Thus, in this study, the Wendland CSRBFs with C4 continuity are adopted:

$$\varphi(r(x, y)) = (\max(0, 1 - r(x, y)))^8 \cdot (35r^2(x, y) + 18r(x, y) + 3) \quad (3)$$

and the radius of support  $r$  is given as:

$$r = \frac{d_I}{R} = \frac{\sqrt{(x - x_i)^2 + (y - y_i)^2}}{R} \quad (4)$$

where  $R$  indicates the radius of influences from the neighbor knots and  $d_I$  means the distance between the two sample knots. It should be pointed out that the radius of support must be determined carefully to satisfy the requirement of interpolation and efficiency of computation.

With regard to the level set function, the CSRBF can be utilized to approximate the

function values at the pre-determined knots within the design space. By introducing a series of RBF kernels and expansion coefficients, the initially time-dependent function can be represented via a continuous parametric form:

$$\Phi(\mathbf{x}, t) = \boldsymbol{\varphi}(\mathbf{x})^T \boldsymbol{\alpha}(t) \quad (5)$$

where  $\boldsymbol{\varphi}(\mathbf{x}) = [\varphi_1(\mathbf{x}), \varphi_2(\mathbf{x}), \dots, \varphi_N(\mathbf{x})]^T$  are the univariate, radially symmetric interpolant kernels, and  $\boldsymbol{\alpha}(t) = [\alpha_1(t), \alpha_2(t), \dots, \alpha_N(t)]^T$  is the expansion coefficient vector.

With the aim of separating the space and time variables in the original Hamilton-Jacobi PDE, the parametric level set function is substituted into Equation (2), which yields:

$$\boldsymbol{\varphi}^T(\mathbf{x}) \frac{d\boldsymbol{\alpha}(t)}{dt} + \mathbf{V}_n \cdot |\nabla \boldsymbol{\varphi}^T(\mathbf{x}) \boldsymbol{\alpha}(t)| = 0 \quad (6)$$

From Equation (6) we can see that the classical level set method has been transformed into a parametric form for solving the topological shape optimization problems. This means the level set-based parameterization approach can simultaneously preserve the attractive features of implicit representation of boundary and replace the time-consuming process of handling Hamilton-Jacobi PDE by solving the rather convenient ODEs.

### 2.3 Interpolant Matrix Compression

We see that even in the CSRBF-based parametric level set method, the computational complexity of interpolation could be quite high for the large-scale optimization problems. Therefore, a DWT-based approximation method is used to solve the system consisting of linear equations arising from CSRBF interpolation. DWT is capable of identifying essential data from a given set of chaotic information, which is widely used in signal processing, image compression, computer vision, etc. This characteristic can be utilized to compress the interpolant matrix in this paper.

Firstly, let us review the parametric level set approach with a matrix representation. All the discrete nodes for the level set function defined in Equation (5) can be given as:

$$\mathbf{A}\boldsymbol{\alpha}^T = \boldsymbol{\Phi}, \text{ where } \boldsymbol{\Phi} = [\Phi_1, \Phi_2, \dots, \Phi_N]^T \quad (7)$$

where  $\mathbf{A}$  is theoretically invertible matrix with the size of  $\mathbf{N} \times \mathbf{N}$ , which can be given as:

$$\mathbf{A} = \begin{bmatrix} \boldsymbol{\varphi}^T(x_1) \\ \boldsymbol{\varphi}^T(x_2) \\ \dots \\ \boldsymbol{\varphi}^T(x_N) \end{bmatrix} = \begin{bmatrix} \varphi_1(x_1) & \varphi_2(x_1) & \dots & \varphi_N(x_1) \\ \varphi_1(x_2) & \varphi_2(x_2) & \dots & \varphi_N(x_2) \\ \dots & \dots & \dots & \dots \\ \varphi_1(x_N) & \varphi_2(x_N) & \dots & \varphi_N(x_N) \end{bmatrix} \quad (8)$$

It should be noticed that one should solve the system  $\boldsymbol{\alpha} = (\mathbf{A}^{-1}\boldsymbol{\Phi})^T$  to obtain the initial values of expansion coefficients at the first iteration, and compute the product  $\mathbf{A}\boldsymbol{\alpha}^T = \boldsymbol{\Phi}$  to determine the discrete values of level set function at the following iterations.

Secondly, we will discuss the implementation of DWT to compress the linear system in Equation (7). To facilitate the illustration, the orthogonal matrix  $\mathbf{W}$  is introduced to transform a vector or matrix with original basis into new one with wavelet basis [15]. Thus, we can

obtain a new system as:

$$\mathbf{W} \cdot \mathbf{A} \cdot (\mathbf{W}^T \cdot \mathbf{W}) \cdot \boldsymbol{\alpha}^T = \mathbf{W} \cdot \boldsymbol{\Phi} \quad (9)$$

where premultiplying  $\mathbf{W}$  on  $\boldsymbol{\alpha}$  and  $\boldsymbol{\Phi}$  means to convert the vector into a wavelet form. Premultiplying  $\mathbf{W}$  as well as postmultiplying  $\mathbf{W}^T$  on both sides of  $\mathbf{A}$  can transform the matrix into its wavelet form.

Further, Equation (9) is simplified as:

$$\bar{\mathbf{A}} \cdot \bar{\boldsymbol{\alpha}}^T = \bar{\boldsymbol{\Phi}} \quad (10)$$

where the three components in Equation (10) are the corresponding wavelet forms for the components in Equation (7).

As stated previously, the new matrix  $\bar{\mathbf{A}}$  only contains few essential coefficients to describe the feature of the whole data set. It means we can eliminate the redundant elements in  $\bar{\mathbf{A}}$  with a proper thresholding method. Here, we adopt the adjustable thresholding scheme specified in [16], which will zero out nearly 99% of elements in  $\bar{\mathbf{A}}$ . For more details about the threshold method, the readers can refer to [16].

After thresholding, the extremely sparse interpolation system can be derived as:

$$\bar{\mathbf{A}}^* \cdot \bar{\boldsymbol{\alpha}}^T = \bar{\boldsymbol{\Phi}} \quad (11)$$

Eventually, the value of level set function and expansion coefficients can be determined by the reconstruction operator as:

$$\boldsymbol{\alpha} = \mathbf{W}^T \cdot \bar{\boldsymbol{\alpha}} \text{ or } \boldsymbol{\Phi} = \mathbf{W}^T \cdot \bar{\boldsymbol{\Phi}} \quad (12)$$

We can expect that the computer storage and the optimization time for the parametric level set-based topological shape optimization method will be remarkable reduced via the applying of CSRBF and DWT.

### 3 MULTI-OBJECTIVE OPTIMIZATION MODEL

With respect to the real-world engineering, many design problems are under the circumstance with multiple loading cases. That is to say, we need to handle a complex multi-objective optimization problem to satisfy the multiple design requirements. Due to the contradictory nature of different objectives, it is impossible to find a unique point to reach the optimality for all the design criterions. An acceptable way is to determine a trade-off point, which is called Pareto solution [17]. As to the topology optimization problem that involves massive design variables, the weighting approaches are regarded as the most rational and effective ones. However, an important defect of these methods lies in that it may fail to capture every Pareto optimal point on non-convex Pareto frontier. Consequently, in this study, the NEWC approach is introduced to describe the multiple objectives. The NEWC can serve as a necessary and sufficient condition for Pareto optimality, and thus it is able to depict the whole Pareto frontier on both convex and non-convex part of Pareto solution set [18,19].

For simplicity, we discuss the stiffness optimization problem for the elastic structure under multiple loading cases. With NEWC, the multi-objective optimization problem can be formulated as:

$$\begin{aligned}
 & \text{Minimize: } J(u, \Phi) = \sum_{k=1}^m (\exp(qw_k) - 1) \exp\left(q \left( \frac{C_k(u, \Phi) - C_k^{\min}}{C_k^{\max} - C_k^{\min}} \right)\right) \\
 & \text{Subject to: } \begin{cases} G(u, \Phi) = \int_D H(\Phi) d\Omega - V^* \leq 0 \\ a(u, \partial u, \Phi) = l(\partial u, \Phi), u|_{\partial\Omega} = u_0, \forall \partial u \in U \end{cases}
 \end{aligned} \tag{13}$$

where the objective for  $k^{\text{th}}$  loading case is given as:

$$C_k(u, \Phi) = \int_D f_k(u) H(\Phi) d\Omega \tag{14}$$

and  $q$  is the exponential constant, which can be set to 2.  $C_k^{\max}$  and  $C_k^{\min}$  represent the utopia points associated with the  $k^{\text{th}}$  load, and are utilized to normalize the objective function to avoid numerical overflow.

#### 4 A SCHEME FOR MANUFACTURING CONSTRAINT

To ensure an optimal design can be fabricated by the extrusion process, it is essentially to maintain the uniform cross sections along the extrusion path. This means the level set values for the knots in the extrusion direction must be kept constant, and numerous extra constraints are added into the formulation given in Equation (13):

$$(\Phi_i = \Phi_j = \dots = \Phi_{ne})_k, \quad k = 1, 2, \dots, K \tag{15}$$

where  $ne$  is the number of elements in the same extrusion path, and  $K$  is the number of elements in a cross section.

Solving an optimization model with massive constraints is not an easy task. Thus, we use an effective heuristic strategy to simplify this model, which is called cross section projection method. The main concept of this approach is demonstrated in Figure 1. We assume the extrusion path is along the  $\mathbf{Z}$  axis. For an individual element  $E_i$ , we firstly aggregate the influences from two types of elements, i.e. the elements in a given neighborhood of  $E_i$  and the elements in the same extrusion path of  $E_i$ . And then, the relative elements are projected onto a 2D plane, which is perpendicular to  $\mathbf{Z}$  axis.

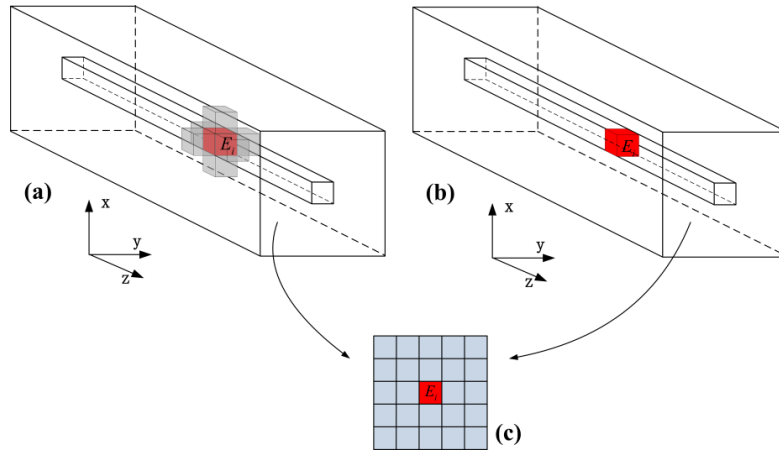


**Figure 1:** Description of cross section projection strategy

For example, the bilinear functional is firstly calculated by considering the influence from the neighborhood:

$$\bar{a}(u, v, \Phi)_i = \frac{1}{\sum_{j=1}^{nae} w(i, j)} \sum_{j=1}^{nae} [w(i, j) (\bar{a}(u, v, \Phi)_i)], \quad (16)$$

$$w(i, j) = rd - dist(i, j).$$

Secondly, we should calculate the bilinear functional once again to aggregate the influence from the same extrusion path:

$$a_p(u, v, \Phi) = \sum_{k=1}^K \left\{ \sum_{i=1}^{ne} \bar{a}(u, v, \Phi)_i / ne \right\}_k \quad (17)$$

In the above two equations,  $nae$  is the number of elements in a given neighborhood of  $E_i$ .  $w$  is the weight coefficient related to the radius of considered neighborhood as well as the distance between adjacent element and  $E_i$ . Via these two operations, one can also achieve an aggregated loading functional similarly.

Eventually, we can convert the 3D optimization problem with extrusion constraint into a 2D projected cross section optimization issue:

$$\begin{aligned} \text{Minimize : } J_p(u, \Phi) &= \sum_{k=1}^m (\exp(qw_k) - 1) \exp \left( q \left( \frac{F_{P,k}(u, \Phi) - F_{P,k}^{\min}}{F_{P,k}^{\max} - F_{P,k}^{\min}} \right) \right) \\ \text{Subject to : } &\begin{cases} G_p(u, \Phi) = \int_{D_p} H(\Phi) d\Omega_p - V_{\max} \leq 0 \\ a_p(u, \partial u, \Phi) = l_p(\partial u, \Phi) \end{cases} \end{aligned} \quad (18)$$

## 5 NUMERICAL EXAMPLES

In this section, we discuss two 3D topology optimization problems under multiple loading cases. The ‘‘ersatz material’’ approach is employed to calculate the strains when the meshes are cut by boundary. We assume that the CSRBF knots are the same with the FEA nodes, and the radius of support for the CSRBF is 3.5. The elastic structure has a Young’s modulus of 180GPa and the Poisson’s ratio is 0.3. The sensitivity analysis for the objective and constraint with respect to the expansion coefficients can be derived via shape derivative method [10]. The optimality criteria (OC) method [1,10] is selected as a solution tool, due to that it is convenient to handle the optimization problems with a large number of design variables and single constraint, which is a classical case in the structural compliance optimization with a linear material volume constraint. We have the optimization terminated when the tolerance  $TOL=10^{-5}$  for the difference of two successive objective values is achieved, or the maximum iteration  $T=200$  is reached. All programs were operated on 2.67GHz Core 2 Duo with 4G Ram.

As given in Figure 2, the design domain is a  $0.3m \times 0.4m \times 1.2m$  beam. Two horizontal edges of the bottom surface of the structure are fixed. There are two loading cases, i.e.  $F1=4kN$  and  $F2=F3=2kN$ , applied at the top face. For simplicity, the weight coefficients are set to  $w1=0.6$  and  $w2=0.4$ , respectively. The design domain is meshed as  $12 \times 16 \times 48$ . The maximum material usage is 0.35. The aim is to determine an optimal structure to minimize

the mean compliances for all loading cases.

We first consider the case without manufacturing constraint. We have  $C_1^{\min} = 122.6412$ ,  $C_1^{\max} = 386.5989$ ,  $C_2^{\min} = 70.3913$  and  $C_2^{\max} = 238.3573$ . By using the proposed parametric level set method, the zeros in interpolation matrix  $\mathbf{A}$ , whose size is  $10829 \times 10829$ , is 98.86%. That is to say, the computational cost will be hugely reduced when comparing to the fully dense matrix. Figure 3 shows the optimization process. We see that several voids have been added in the initial design. After drastically topological changes and shape variation, the optimal result plotted in Figure 3(d) was achieved. Apparently, it cannot be manufactured by the extrusion process. The convergent histories of the mean compliances for different loading cases and the structural volume constraint are plotted in Figure 4. It takes 200 iterations achieve the optimal value (3.59149) of objective function. Accordingly, the mean compliance is 124.3012 for the first loading case and is 73.8715 for the second loading case. The CPU-time of the optimization is approximately 253.46s per iteration.

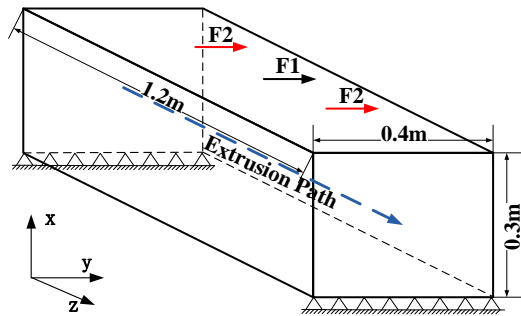


Figure 2: Design domain

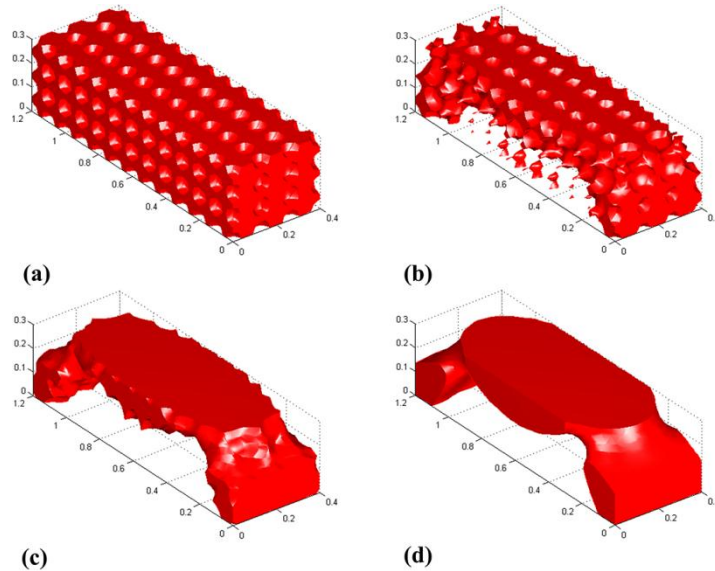
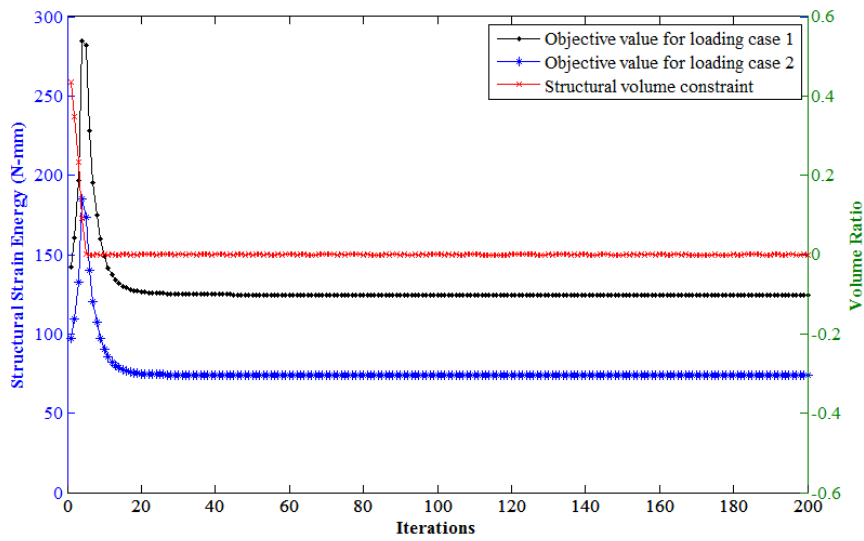
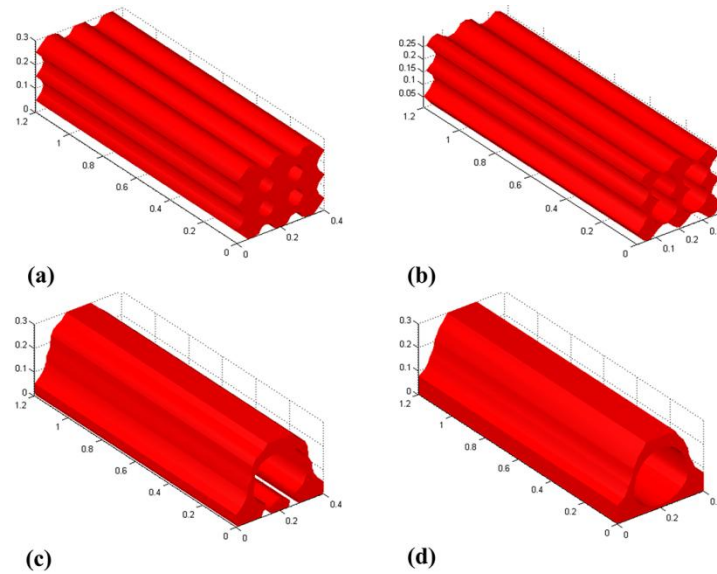


Figure 3: Optimization process for the case without extrusion constraint: (a) initial design; (b) intermediate design; (c) intermediate design; (d) optimal design.



**Figure 4:** Convergent history for the case without extrusion constraint.



**Figure 5:** Optimization process for the case with extrusion constraint: (a) initial design; (b) intermediate design; (c) intermediate design; (d) optimal design.

Then, we consider the case with extrusion constraint. As shown in Figure 2, the extrusion path is along the  $Z$  axis. The boundary and FEA meshes are the same as first example. We have  $C_1^{\min}=197.7915$ ,  $C_1^{\max}=1741.5835$ ,  $C_2^{\min}=127.2671$  and  $C_2^{\max}=1305.6066$ . In fact, with the cross section projection method, the optimization process is worked in a 2D space with  $12 \times 16$  meshes. Figure 4 shows the optimization process of the second example. We see that the cross sections along an extrusion path are kept constant during iterations, and the final design can be fabricated by the extrusion process. The convergent histories of the mean compliances for different loading cases and the structural volume constraint are plotted in

Figure 6. The optimization takes 110 steps, and the optimal value of objective function is 3.57716. The final compliances for the two loading cases are 200.7924 and 137.9703, respectively. The average CPU time is 163.64s per step.

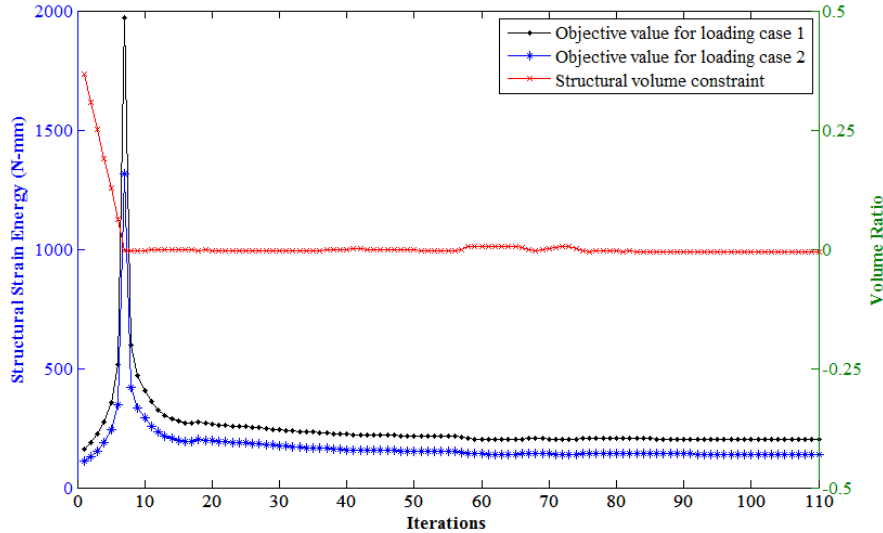


Figure 6: Convergent history for the case with extrusion constraint.

## 6 CONCLUSIONS

This paper proposed a parametric level set method for the topological shape optimization design of the extrudable structures under multiple loading cases. The DWT has been incorporated into the framework of CSRBF-based level set method. An extremely sparse interpolant system was observed, and thus the computational cost had been reduced. The cross section projection strategy was also included to satisfy the extrusion constraint. Finally, the NEWC method has been introduced to model the multi-objective optimization problems. Numerical examples verified the efficiency of proposed approach.

## ACKNOWLEDGMENTS

This work is supported by the National Natural-Science-Foundation-of-China (NSFC) (51175197 and 51305147).

## REFERENCES

- [1] Rozvany, G.I.N. A critical review of established methods of structural topology optimization. *Struct. Multidiscip. Opt.*(2008)**37**:217-237.
- [2] Bendsoe, M.P. and Kikuchi, N. Generating optimal topology in structural design using a homogenization method. *Comput. Methods Appl. Mech. Engrg.*(1988)**71**:197-224.
- [3] Zhou, M. and Rozvany, G.I.N. The COC algorithm. Part II: Topological, geometry and generalized shape optimization. *Comput. Methods Appl. Mech. Engrg.*(1991)**89**:197-224.
- [4] Bendsoe, M.P. and Sigmund, O. Material interpolation schemes in topology optimization. *Arch. Appl. Mech.*(1999)**69**:635-654.

- [5] Xie, Y.M. and Steven, G.P. A simple evolutionary procedure for structural optimization. *Comput. Struct.*(1993)**49**:885-896.
- [6] Sethian, J.A. and Wiegmann, A. Structural boundary design via level set and immersed interface methods. *J. Comput. Phys.*(2000)**163**:489-528.
- [7] Wang, M.Y., Wang, X.M. and Guo, D.M. A level set method for structural topology optimization. *Comput. Methods Appl. Mech. Engrg.*(2003)**192**:227-246.
- [8] Allaire, G., Jouve, F. and Toader, A.M. Structural optimization using sensitivity analysis and a level-set method. *J. Comput. Phys.*(2004)**194**:363-393.
- [9] Yamada, T., Izui, K., Nishiwaki, S. and Takezawa, A. A topology optimization method based on the level set method incorporating a fictitious interface energy. *Comput. Methods Appl. Mech. Engrg.*(2010)**199**:2876-2891.
- [10] Luo, Z., Wang, M.Y., Wang, S. and Wei, P. A level set-based parameterization method for structural shape and topology optimization. *Int. J. Numer. Meth. Eng.*(2008)**76**:1-26.
- [11] Wendland, H. Piecewise polynomial, positive definite and compactly supported radial functions of minimal degree. *Adv. Comput. Math.*(1995)**4**:389-396.
- [12] Kim, Y.Y. and Kim, T.S. Topology optimization of beam cross sections. *Int. J. Solids Struct.*(2000) **37**:477-493.
- [13] Ishii, K. and Aomura, S. Topology optimization for the extruded three dimensional structure with constant cross section. *JSME Int. J. Ser. A-Solid Mech. Mater. Eng.* (2004)**47**:198-206.
- [14] Patel, N.M., Penninger, C.L. and Renaud, J.E. Topology synthesis of extrusion-based nonlinear transient designs. *ASME J. Mech. Des.*(2009)**131**:061003.1-061003.11.
- [15] Chen, K. Discrete wavelet transforms accelerated sparse preconditioners for dense boundary element systems. *Electron. T. Numer. Ana.*(1999)**8**:138-153.
- [16] Ravnik, J., Škerget, L. and Hriberšek, M. The wavelet transform for BEM computational fluid dynamics. *Eng. Anal. Bound. Elem.*(2004)**28**:1303-1314.
- [17] Marler, R.T. and Arora, J.S. Survey of Multi-objective Optimization Methods for Engineering. *Struct. Multidiscip. Opt.*(2004)**26**:369-395.
- [18] Marler, R.T. and Arora, J.S. The Weighted Sum Method for Multi-objective Optimization: New Insights. *Struct. Multidiscip. Opt.*(2009)**41**:853-862.
- [19] Li, H., Gao, L. and Li, P.G. Topology optimization of structures under multiple loading cases with a new compliance-volume product. *Eng. Optimiz.*(2014)**46**:725-744.